

# Beam shaping based on intermediate zone diffraction of a micro-aperture

DANYAN ZENG, ZHIJUN SUN\*

Department of Physics, Xiamen University, Xiamen 361005, China

\*Corresponding author: sunzj@xmu.edu.cn

We analyze optical diffraction of a micro-aperture (slit or hole) in a metal screen in the intermediate zone and report its application for beam focusing and collimating in micro-optics. Both finite-difference time-domain simulations and Rayleigh–Sommerfeld diffraction formula were applied to calculate the intermediate-zone diffraction patterns. It is shown that, by controlling the aperture size, the focal length and depth can be adjusted in a very wide range, from subwavelength to tens of wavelengths, while the focal width maintains in an order of wavelength.

Keywords: aperture, diffraction, beam shaping.

## 1. Introduction

The study of optical diffraction/scattering of apertures has a long history [1–4]. Considering the size of an aperture ( $a \ll \lambda$ ,  $a \sim \lambda$ ,  $a \gg \lambda$ ) and position of an observation point (near field zone  $R \ll \lambda$ , intermediate field zone  $R \sim \lambda$ , far field zone  $R \gg \lambda$ ), diffraction can be categorized according to the different kinds. Being of interest, far field diffractions have been elaborately studied for both large apertures (known as Fraunhofer diffraction or Fresnel diffraction [4]) and small apertures ( $a \sim \lambda$ ) [5, 6]. Theories based on assumptions and proper approximations accurately describe far field diffractions in elegant expressions [4–7]. For a tiny aperture ( $a \ll \lambda$ ), near field electro-optical interactions are in the focus of the study, where finite conductivity of the metal of the opaque plane has to be considered [2, 6, 8]. And recently, optical transmission through such a tiny aperture or periodically arrayed apertures has been the subject of extensive research [9–11]. Nowadays, dimensions of integrated optical devices have reached a scale of tens of micrometers in micro-optical systems; further miniaturization will involve the intermediate zone diffraction of small apertures ( $\sim$  micrometers). In analyzing such diffractions, effects of near field interactions will have to be considered.

In this work, firstly we analyze the diffraction of a small slit in a metal plane with finite-difference time-domain (FDTD) numerical method, which rigorously solves

the problem based on Maxwell's equations and Drude model of metal. Both TE (electric field is parallel with slit) and TM (magnetic field is parallel with slit) polarizations at normal incidence are simulated and compared with those obtained with the scalar-field Rayleigh–Sommerfeld (R–S) diffraction formula [12]. Diffraction patterns with local maxima of different orders are observed in the intermediate zone. Of particular interest is the 0th-order diffraction in this zone, which offers strong potential for beam focusing or collimating applications in micro-optics. The effect/function can then be extended to micro-apertures considering practically insensitivity of field patterns to polarization in the intermediate zone.

## 2. Optical diffraction of a micro-aperture in the intermediate zone

Figure 1 shows FDTD calculated distribution of average intensity of diffracted light normally incident on a slit of varying widths ( $a = \lambda, 2\lambda, 3\lambda, 4\lambda$ ) in a metal (Ag) film in TE/TM polarizations, which are compared with those calculated with scalar-field R–S diffraction formula. In the FDTD analysis, finite conductivity of the metal (Ag) is embodied in a Drude model ( $\varepsilon(\omega) = \varepsilon_\infty - \omega_p^2 / (\omega^2 + i\gamma\omega)$ ) fit of its experimental permittivity [13]. The thickness of the metal screen is 100 nm, discretized with the grid size of 10 nm. An optical plane wave of 600 nm wavelength is normally incident onto the screen. Since normalized units ( $\tilde{\mathbf{E}} = \sqrt{\varepsilon_0 / \mu_0} \mathbf{E}$ ) [14] and same incidence field amplitude of unity have been used, the calculated FDTD absolute values of intensity in Fig. 1 should be comparable for both polarizations. In calculations with scalar R–S formula [12], the kernel function was replaced with  $G_0 = \exp(ikR) / \sqrt{R}$  for the 2-dimensional cylindrical waves, *i.e.*, the scalar field

$$\phi(x, y) = \frac{k}{\pi i} \int_{y=0} \phi(x', 0) \frac{\mathbf{n}' \cdot \mathbf{R}}{R} \left( 1 + \frac{i}{2kR} \right) \frac{\exp(ikR)}{\sqrt{R}} dx' \quad (1)$$

at the observation points. The corresponding intensity is  $I = \phi \phi^*$ . Here,  $k = 2\pi/\lambda$ ,  $\mathbf{R}$  is a vector from point  $(x', 0)$  in the slit plane to the observation point  $(x, y)$  ( $z$  direction is perpendicular to the paper plane),  $\mathbf{n}'$  is the unit normal vector of the slit plane. The field magnitude  $\phi(x', 0)$  within the slit is considered as that of an unperturbed incidence wave as usual. But it will be shown that a field distribution equivalent to the perturbed one in reality can be self-constructed by evolution of the unperturbed one within a very short spatial shift.

From Figure 1, one can observe similarity of the local diffraction patterns in the intermediate zone for TE/TM polarizations and those calculated from scalar R–S formula. A further examination indicates larger transmissivity for TE polarization incidence. It is contrary to the case for very narrow slits ( $a \ll \lambda$ ), in which surface wave of plasmons excited at the slit enhances transmission of TM polarized incidence light, while it is within a cut-off of waveguiding for TE polarization. Here, the induced  $E_y$ -field in the TM case generates surface waves on the metal plane, which bring more absorption and result in the transmission reduction (shown in Fig. 2 as an example). If

neglecting the near field effects, diffraction of a slit can be considered as a superposition of forward transmitting waves and perturbation waves induced by the edges. In the results shown in Fig. 1, the perturbed field near the slit exit has  $M = \text{Int}(a/\lambda)$  maxima of intensity, different from that of standing wave type interference forming

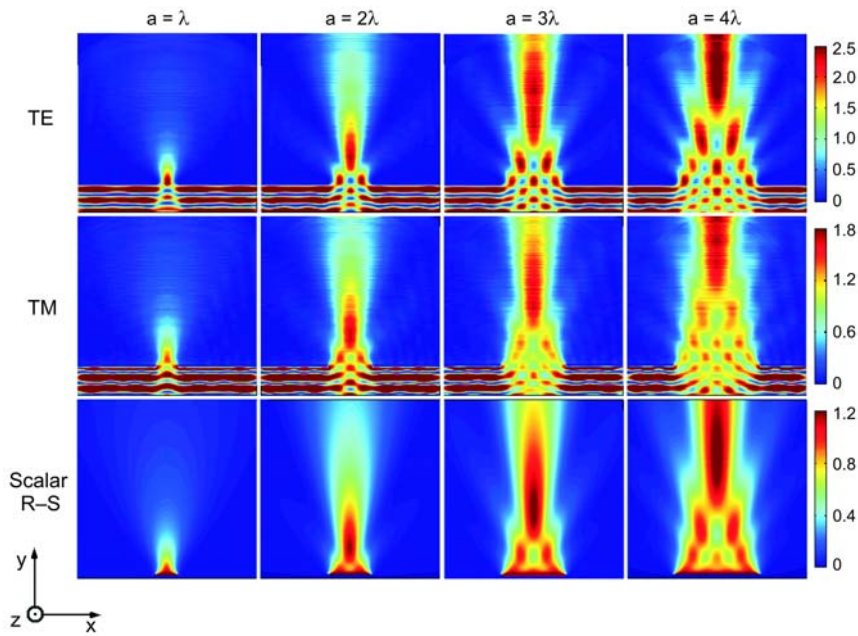


Fig. 1. FDTD simulated average intensity distributions of light diffracted by slits of varying widths in a metal (Ag) film for TE and TM polarizations, compared with those calculated with scalar R-S formula. In FDTD simulations, the thickness of the metal film is 100 nm, and the plane wave of 600 nm wavelength is normally incident onto both the screen and the slit. Images of each column have the same slit widths as indicated above of the set of photos, and each row corresponds to TE or TM polarization in FDTD simulations or scalar analysis with R-S formula. Each colorbar is applied to images of the same row. Sizes of all the images are the same ( $5 \times 5 \mu\text{m}^2$ ).

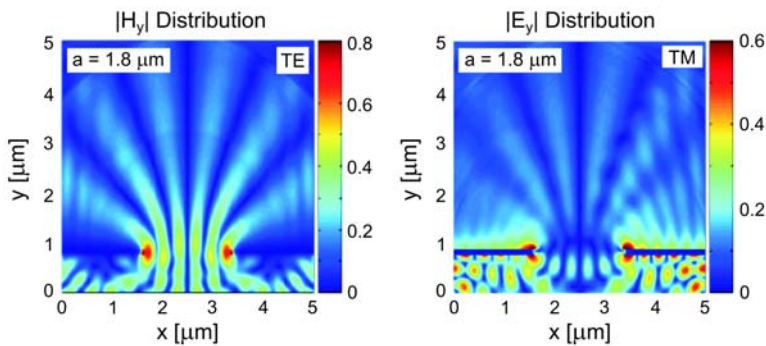


Fig. 2. Distributions of  $H_y$  (or  $E_y$ ) field amplitude for a slit of width  $3\lambda$  under illumination of TE (or TM) polarized light. The plane wave of wavelength  $\lambda = 600 \text{ nm}$  is incident from the bottom side of each image.

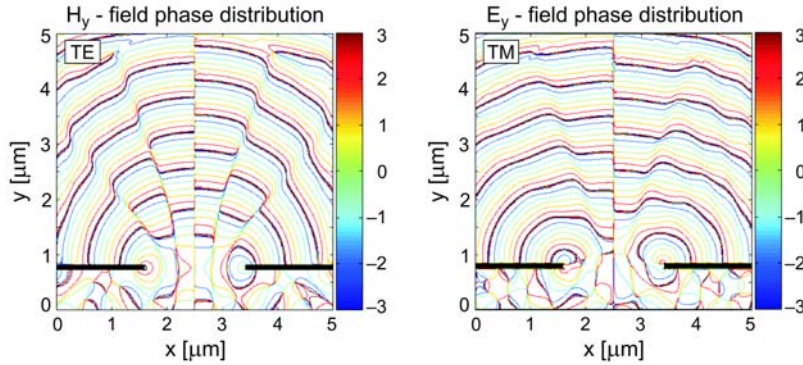


Fig. 3. Instant phase distributions of partial fields for a slit of width  $3\lambda$  under illumination of TE (or TM) polarized light. The plane wave of wavelength  $\lambda = 600$  nm is incident from the bottom side of each image.

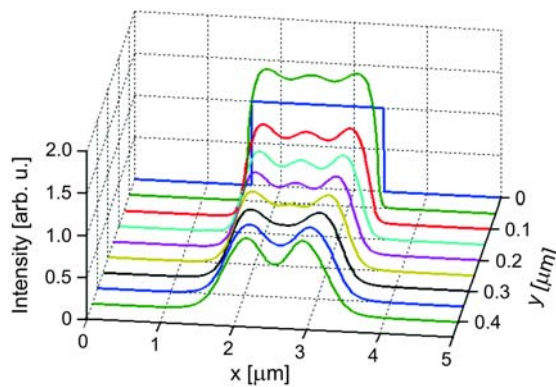


Fig. 4. A zoom-in line plot of the diffraction intensity distribution near the secondary source line of a slit calculated with R-S formula, which shows self-construction of equivalent perturbed field in evolution of the secondary source with finite width. The corresponding slit width is  $1.8 \mu\text{m}$  and the wavelength is  $600$  nm.

between the edge boundaries, which correspond to  $2M$  maxima in principle. As it propagates forward through the slit, it evolves into degressive numbers ( $M - 1$ ,  $M - 2$ , ...,  $1$ ) of maxima in the intermediate zone, which relate to far field diffraction beams of the same orders. Among the local maxima in the intermediate zone, the 0th-order shows strong confinement of transmitted power in the transverse direction and there is a notable extent in the longitudinal direction. This property might be used for beam shaping in the micro-optics regime.

We also calculated phase distributions of partial fields with FDTD simulations in Fig. 3. It is interesting to find that the geometric symmetry results in antisymmetric phase distributions of the induced fields  $E_y$  (for TM) and  $H_y$  (for TE) with respect to the middle line. There are directions that transverse differentiation of phase of the field  $E_y$  (for TM) or  $H_y$  (for TE) is large or abrupt (singular). It is shown, in Fig. 2, that

amplitudes of the partial fields appear minimal in such directions; while diffraction intensity in these directions takes its maxima in far field.

As for calculation with the R–S formula, it neglects perturbation on initial field within the aperture and near field interactions at the metal screen surfaces. The dependence of diffraction on polarization is subject to the near field effects. As the slit is larger than incidence wavelength, the near field effects are not dominant, especially for the 0th-order diffractive transmission. It is also found that, although an unperturbed field in the slit is assumed in the calculations, an equivalent edge diffraction effect can result by the assumed finite secondary sources (see Fig. 4). Self-construction of “perturbed” field shows effect immediately in an infinitesimal shift from the source line. Notice that it is just the result of implementation of R–S formula (Eq. (1)); for the far field ( $R \gg \lambda$ ) case, the equation evolves into an approximation of Fourier transform. Self-construction of the perturbed field in the aperture discloses the historical issue of how false assumptions of the diffraction theory (Kirchhoff’s theory, or in Rayleigh–Sommerfeld form) lead to correct predictions. From comparison with FDTD simulations, it also suggests that the scalar formula cannot only be applied for diffraction of large apertures and far field diffractions, it also works well in the intermediate zone for a small aperture of dimension in the order of wavelength.

### 3. Performance of a micro-slit/hole lens for beam forming

We further evaluated the beam focusing of the 0th-order maxima for wider slits of interest (up to ten wavelengths). It was found, as shown in Fig. 5, that the focal length (distance of maxima to slit screen) can extend to a range of tens of wavelengths, while the focal width (defined with full-width-half-maximum, FWHM) maintains within a few wavelengths. The focal depth (defined as the spacing between a 10% drop from the focal maximum in the forward direction) also varies in a range from subwavelength to tens of wavelengths with the widening of the slit. Thus, for a narrower slit, it works better as a focusing lens; for a wider slit, it can also work as a collimator. The collimated beam was shown to have nearly plane wave fronts and Gaussian distribution of intensity in transverse direction. In extrapolation, for large slits ( $a \gg \lambda$ ), the focal depth approaches infinity, the diffraction principal maxima of which in far field appear transversely well confined and nearly uniform in propagation direction. But for small slits, far field diffraction is far away from the maxima near slit, thus it is highly attenuated.

Note that, although the above analysis is based on the wavelength of 600 nm, the results can be scaled with the wavelength and generalized in that the near field effects are negligible for intermediate zone diffraction from the point of view of applications. The scalar analysis can also be applied to apertures of rectangular and circular shape, where the kernel equation is taken for spherical waves [12],  $G_0 = \exp(ikR)/R$ . Well-defined beam focusing is observed, as shown in Fig. 6. Notice that,

for rectangular aperture of size within a few wavelengths, it needs to be square to avoid mismatching of focus for orthogonal directions of diffraction. It is worth mentioning that such intermediate zone diffraction pattern of a small aperture is very similar to that of a small sphere, which also shows some focusing effect [15]. But the small aperture shows obvious advantages in flexibilities of design, manufacturing and functioning, *e.g.*, in integration with other photonic or optoelectronic arrayed devices. For conventional micro-optic lens, as its dimensions are reduced to a scale of

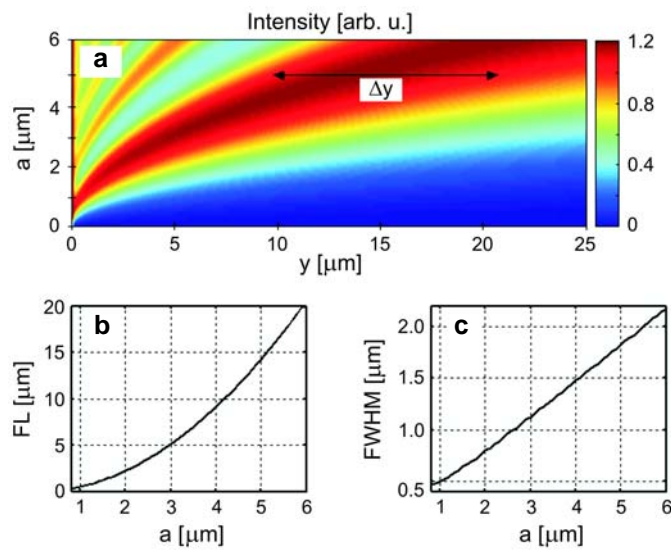


Fig. 5. Dependence of beam focusing parameters on slit width calculated with R–S formula. A colormap of intensity along the middle line of forward propagating beam for different slit widths (a). Dependence of focal length (FL) on slit width (b). Dependence of FWHM focal width on slit width (c). The label  $\Delta y$  in (a) indicates focal depth of 11  $\mu\text{m}$  for slit width of 5  $\mu\text{m}$ . The reference wavelength is 600 nm in calculations.

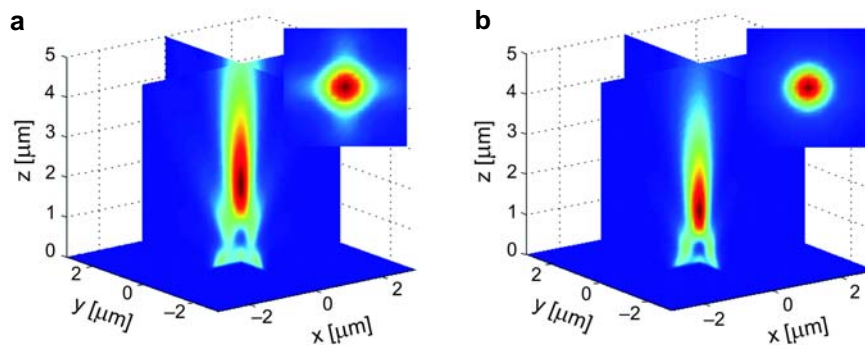


Fig. 6. Sliced 3D images of intermediate zone diffraction patterns of rectangular ( $1.8 \times 1.8 \mu\text{m}^2$ ) – a, and circular (1.8  $\mu\text{m}$  in diameter) – b apertures. Wavelength of normal incidence plane wave is 600 nm. Inset of each image is a transverse cross-section display of intensity distribution at the focal point.

micrometers, it fails to function because of edge diffraction and micro-cavity effects. If it is to achieve the same level of performance with high numerical aperture (NA) micro-optic lens, the integration density will have to be reduced, far less comparable with a lens array of just micrometers-spaced apertures.

#### 4. Conclusions

By analyzing the intermediate zone diffraction of a small aperture, we proposed some type of optical beam shaping lens consisting of just a micro-aperture for beam focusing and collimating for ultra-compact micro-optic applications. By controlling the aperture size, the focal length and depth can be adjusted in a very wide range, from subwavelength to tens of wavelengths, while the focal width maintains narrow within an order of wavelength. The functions can also be extended to other spectrum regime of electromagnetic waves.

*Acknowledgements* – This work was supported by National Natural Science Foundation of China (No. 60707012), Natural Science Foundation of Fujian Province of China (No. A0710019) and the NCETFJ program in China.

#### References

- [1] RAYLEIGH L., *On the passage of waves through apertures in plane screens, and allied problems*, Philosophical Magazine **43**, 1897, pp. 259–72.
- [2] BETHE H.A., *Theory of diffraction by small holes*, Physical Review **66**(7–8), 1944, pp. 163–82.
- [3] BOUWKAMP C.J., *Diffraction theory*, Reports on Progress in Physics **17**, 1954, pp. 35–100.
- [4] BORN M., WOLF E., *Principles of Optics*, 7th Ed., Cambridge University Press, 1999.
- [5] STRATTON J.A., CHU L.J., *Diffraction theory of electromagnetic waves*, Physical Review **56**(1), 1939, pp. 99–107.
- [6] SMYTHE W.R., *The double current sheet in diffraction*, Physical Review **72**(11), 1947, pp. 1066–70.
- [7] JACKSON J.D., *Classical Electrodynamics*, 3rd Ed., Wiley, New York, 1998, Chap. 10.
- [8] SCHOUTEN H.F., VISSER T.D., LENSTRA D., BLOK H., *Light transmission through a subwavelength slit: Waveguiding and optical vortices*, Physical Review E **67**(3), 2003, p. 036608.
- [9] GIRARD C., DEREUX A., *Near-field optics theories*, Reports on Progress in Physics **59**(5), 1996, pp. 657–99.
- [10] EBBESEN T.W., LEZEC H.J., GHAEMI H.F., THIO T., WOLFF P.A., *Extraordinary optical transmission through sub-wavelength hole arrays*, Nature **391**(6668), 1998, pp. 667–9.
- [11] SUN Z., JUNG Y.S., KIM H.K., *Role of surface plasmons in the optical interaction in metallic gratings with narrow slits*, Applied Physics Letters **83**(15), 2003, pp. 3021–3.
- [12] JACKSON J.D., *Classical Electrodynamics*, 3rd Ed., Wiley, New York, 1998, p. 481.
- [13] PALIK E.D. [Ed], *Handbook of Optical Constants of Solids*, Academic, New York, 1998.
- [14] SULLIVAN D.M., *Electromagnetic Simulation Using the FDTD Method*, IEEE Press, New York, 2000.
- [15] KOFLER J., ARNOLD N., *Axially symmetric focusing as a cuspid diffraction catastrophe: Scalar and vector cases and comparison with the theory of Mie*, Physical Review B: Condensed Matter and Materials Physics **73**(23), 2006, p. 235401.

*Received January 17, 2008*